

Cross sections for resonant vibrational excitation of N_2 by electron impact

A. U. Hazi, T. N. Rescigno, and M. Kurilla

Theoretical Atomic and Molecular Physics Group, Lawrence Livermore National Laboratory, University of California, Livermore, California 94550

(Received 22 September 1980)

We report the results of a theoretical study of resonant vibrational-excitation of N_2 by low-energy electrons. The vibrational-excitation cross sections were calculated using *ab initio* fixed-nuclei resonance parameters in the complex-potential or "boomerang" model of Dubé and Herzenberg. The electronic resonance energy and decay width were extracted from several *ab initio* calculations of the ${}^2\Pi_g$ shape resonance of N_2^- . The good agreement between the present cross sections and those obtained recently with the *R*-matrix technique indicates that the assumptions underlying the complex-potential model are valid for the case of $N_2^-({}^2\Pi_g)$. The present results also show the sensitivity of the computed vibrational-excitation cross sections to the fixed-nuclei resonance parameters employed in the calculations. The differential vibrational-excitation cross sections at 90° and the total integrated cross section which we have obtained agree reasonably well with the available experimental data.

I. INTRODUCTION

It is well known that the scattering of low-energy electrons by molecules is often dominated by negative-ion shape resonances. In most cases, such resonances lead to relatively large cross sections for vibrational-excitation and dissociative attachment, and therefore play an important role in electrically excited gas lasers, various discharges, and electron transport through the upper atmosphere. The ${}^2\Pi_g$ resonance of N_2^- is perhaps the most widely known example: The resonant vibrational excitation of N_2 between 1 and 5 eV has been studied extensively both experimentally¹⁻³ and theoretically.⁴⁻¹¹

During the past ten years several theoretical methods have been proposed for calculating directly resonant vibrational-excitation cross sections of simple molecules: The complex-energy or "boomerang" method,^{5,6} the energy-modified adiabatic approximation,⁷ a many-body harmonic oscillator approximation,⁸ the vibrational close-coupling method^{9,10} and, most recently, the *R*-matrix technique.^{11,12} All of these methods, except the vibrational close-coupling approach, utilize some form of the Born-Oppenheimer approximation for separating the electronic and nuclear motions. As a result, the vibrational motion of the nuclei is described in terms of electronic parameters (potential-energy curves and decay widths) which depend parametrically on the internuclear distance, and which can be extracted, in principle, from *ab initio*, electron-molecule scattering calculations done with fixed nuclei. Nevertheless, all previous applications of the boomerang model to vibrational excitation,^{5,6,13} as well as to dissociative attachment,^{13,14} have used a semiempirical approach in which the electronic resonance parameters are adjusted to obtain agreement with a portion of the

experimental data. For example, Dubé and Herzenberg⁶ determined a parametrized complex potential curve for $N_2^-({}^2\Pi_g)$ from the energy dependence of the differential cross section for the $v=0 \rightarrow 1$ excitation at 90° .³ Once the adjustable parameters were fixed, they computed absolute cross sections for excitation of the $v=1, 2, 3$ levels of N_2 and obtained satisfactory agreement with the available experimental data. Other calculations^{7,8,13} used similarly determined resonance parameters.

On the other hand, *ab initio* calculations of the resonant vibrational-excitation cross sections for N_2 had mixed success. Purely fixed-nuclei calculations¹⁵ provide excitation cross sections without any structure, and the neglect of target polarization usually yields a resonance position which is ~ 2 eV too high.¹⁶ The vibrational close-coupling calculation of Chandra and Temkin^{9,10} gave cross sections in which vibrational structure appeared at the right scattering energy. However, their close-coupling expansions were apparently not fully converged¹⁷ and consequently their vibrational-excitation cross sections are only qualitatively correct. More recently, Schneider, LeDourneuf, and Vo Ky Lan¹¹ obtained good agreement with experimental cross sections by using the Born-Oppenheimer approximation combined with an *R*-matrix approach.¹² The electron scattering from a fixed target was treated using the static-exchange potential of a polarized N_2 molecule, whereas the vibrational motion of the N_2^- compound state was described by an *R*-matrix formulation.¹² This calculation clearly demonstrated for the first time that a properly chosen *ab initio* method is capable of providing accurate cross sections for resonant vibrational excitation of diatomic molecules by electron impact.

In this paper we show that equally accurate vibrational-excitation cross sections can be calcula-

ted using the complex-potential or boomerang model⁶ with electronic resonance parameters determined *ab initio*. To our knowledge, this work constitutes the first application of this model to vibrational excitation where the required complex potential-energy curve of the negative-ion shape resonance was derived from *ab initio* fixed-nuclei electron-scattering calculations. In addition, we studied the validity of the assumptions underlying the complex-potential model for describing vibrational motion, and examined the dependence of the computed excitation cross sections on the accuracy of the electronic resonance parameters employed in the calculations. Our results show that, in the case of $N_2^-(^2\Pi_g)$, the assumption of a local resonance width $\Gamma(R)$ is justified. We also confirm the previous finding^{11,16} that polarization of the target molecule must be properly described in order to obtain the correct magnitude and energy dependence of the vibrational-excitation cross sections. We show that the detailed structure of the computed cross sections is rather sensitive to the potential-energy curve (resonance energy) of the negative-ion compound state.⁶ On the other hand, the width of the resonance controls mostly the overall magnitude of the cross section. A comparison of the calculated and the experimental total cross sections^{2,18} for N_2 suggests that the boomerang model provides a vibrationally elastic ($v=0 \rightarrow 0$), $^2\Pi_g$ partial cross section which is much less satisfactory than the corresponding inelastic cross sections.

In the remainder of the paper, Sec. II contains a derivation of the complex-potential or boomerang model for vibrational motion, and Sec. III describes the fixed-nuclei electronic resonance parameters (energies and widths) which were used in the present calculations. In Sec. IV we present the computed vibrational-excitation cross sections and compare them to some previous theoretical and experimental results. Finally, Sec. V summarizes our conclusions.

II. COMPLEX-POTENTIAL OR BOOMERANG MODEL FOR RESONANT ELECTRON-MOLECULE SCATTERING

Shortly after resonances of molecular negative ions were discovered, the complex-potential or boomerang model was introduced^{5,19} to describe the motion of the nuclei during electron-molecule collisions. Originally, the model was adapted from the Kapur-Peierls theory of resonant scattering.²⁰ By using the Born-Oppenheimer separation of electronic and nuclear motions, the model assumes that the incident electron is captured into a quasistationary state of the molecular negative ion $\Psi_r(\vec{r}, R)$, where \vec{r} represents the electronic co-

ordinates and R is the internuclear distance. Since the electron can autodetach, the resonance state has a finite lifetime $\hbar/\Gamma(R)$, where $\Gamma(R)$ is called the electronic resonance width. Vibrational excitation of the nuclei is enhanced if the electron is trapped for at least one vibrational period.

In the following, we give a brief derivation of the differential equation which governs the relative motion of the nuclei in order to identify the major assumptions underlying the model. Using formal resonance scattering theory,²¹ one can show that, for vibrational excitation $v_i \rightarrow v_f$, the "resonant" part of the T matrix is given by

$$T_{v_f, v_i} = \langle P\phi_{v_f}^- PHQ\bar{\Psi}_{v_i}^+ \rangle, \quad (1)$$

where the operator Q projects onto the resonance state, and $Q+P=1$, $QP=0$. The total molecular Hamiltonian H has the form

$$H(\vec{r}, \vec{R}) = H_{e1}(\vec{r}, R) + K_R, \quad (2)$$

where K_R is the kinetic energy operator for the nuclei, and $H_{e1}(\vec{r}, R)$ is the electronic Hamiltonian for fixed internuclear distance R . The "nonresonant" scattering solutions $P\phi_{v_f}^+$ satisfy the equation

$$(E - PHP)P\phi_{v_f}^+ = 0 \quad (3)$$

and have the usual boundary conditions. The resonant wave function $Q\bar{\Psi}_{v_i}^+$ satisfies the equation

$$(E - QHQ)Q\bar{\Psi}_{v_i}^+ = QHP(P\phi_{v_i}^+ + G_p^+ PHQ\bar{\Psi}_{v_i}^+), \quad (4)$$

where

$$G_p^+ = \frac{1}{E^+ - PHP}. \quad (5)$$

Now we assume that there is a single isolated electronic resonance state with a normalized wave function $\psi_r(\vec{r}, R)$ and energy $\epsilon_r(R) = (\psi_r(\vec{r}, R)H_{e1}(\vec{r}, R) \times \psi_r(\vec{r}, R))$, where the bold parentheses imply integration over only the electronic coordinates. If we define

$$Q = \psi_r(\vec{r}, R)\langle \psi_r(\vec{r}, R), \quad (6)$$

then

$$Q\bar{\Psi}_{v_i}^+ = \psi_r(\vec{r}, R)\xi_{v_i}(\vec{R}), \quad (7)$$

where the function $\xi_{v_i}(\vec{R})$ describes the relative motion of the nuclei in the negative-ion compound state. Next, we assume that the Born-Oppenheimer approximation is valid both for the resonance state $\psi_r(\vec{r}, R)$ and for the nonresonant scattering solutions $P\phi_{v_i}^+$. Consequently,

$$[K_R, Q] = [K_R, P] = 0 \quad (8a)$$

and

$$QK_R P = PK_R Q = 0. \quad (8b)$$

Equation (8b) implies that the coupling between the resonance and the background continuum is due to electronic interactions only. By multiplying Eq. (4) with $\psi_r(\vec{r}, R)^*$, then integrating over the electronic coordinates, and using Eqs. (7) and (8), we obtain

$$[E - \epsilon_r(R) - K_R] \xi_{v_i}(\vec{R}) = (\psi_r H_{e1} P \phi_{v_i}^*) + (\psi_r H_{e1} P G_p^* P H_{e1} \psi_r) \xi_{v_i}(\vec{R}). \quad (9)$$

To simplify Eq. (9), one can use the spectral representation of G_p^* implied by Eqs. (3) and (5):

$$[E - \epsilon_r(R) - K_R] \xi_{v_i}(\vec{R}) = U_{E v_i}(\vec{R}) + \sum_v \mathcal{P} \int dE' \frac{U_{E' v}(\vec{R})}{E - E'} \int d\vec{R}' U_{E' v}^*(\vec{R}') \xi_{v_i}(\vec{R}') - (i\pi) \sum_v U_{E v}(\vec{R}) \int d\vec{R}' U_{E v}^*(\vec{R}') \xi_{v_i}(\vec{R}'). \quad (10)$$

In Eq. (10), $\mathcal{P} \int dE'$ implies a principal value integral and the sum v runs over the open vibrational channels.

The matrix element

$$U_{E v}(\vec{R}) = (\psi_r(\vec{r}, R) H_{e1} P \phi_{E v}^*(\vec{r}, R))$$

represents the coupling between the resonance state and the nonresonant solution $P \phi_{E v}^*$ associated with energy E and vibrational state v . The quantities $U_{E v_i}$ and $U_{E v_f}$ are called the entry and exit amplitudes, respectively.^{5,6} Equation (10) is exact within the Born-Oppenheimer approximation, and it determines the nuclear wave function $\xi_{v_i}(\vec{R})$ associated with the resonance state.²² Unfortunately, it also contains a complex nonlocal integral operator because of the presence of the nuclear kinetic energy operator in G_p^* [Eq. (5)].

In order to simplify Eq. (10) further, several additional assumptions are necessary. First, we assume that the adiabatic nuclei approximation^{23,24} is valid for the nonresonant part of the electron-molecule scattering. As a result, $P \phi_{E v}^*$ can be written as a product of electronic and nuclear wave functions, i.e.,

$$P \phi_{E v}^*(\vec{r}, \vec{R}) = \psi_{k_v}^*(\vec{r}, R) X_v(\vec{R}). \quad (11)$$

The fixed-nuclei electronic-scattering function satisfies the equation

$$[P H_{e1}(\vec{r}, R) P - \frac{1}{2} k_v^2] \psi_{k_v}^*(\vec{r}, R) = 0 \quad (12)$$

with $E = \frac{1}{2} k_v^2 + W_v$ where W_v is the energy of the v th vibrational-rotational state of the target molecule.

The corresponding nuclear wave function $X_v(\vec{R})$ is a solution of the equation

$$[K_R + \epsilon_0(R) - W_v] X_v(\vec{R}) = 0, \quad (13)$$

where $\epsilon_0(R)$ is the usual Born-Oppenheimer electronic potential-energy curve of the target.²⁵ By substituting Eq. (11) into the expression for $U_{E v}(\vec{R})$ we obtain

$$U_{E v}(\vec{R}) = (\psi_r(\vec{r}, R) H_{e1} \psi_{k_v}^*(\vec{r}, R)) X_v(\vec{R}). \quad (14)$$

At fixed internuclear distance R , the resonance width for ejecting an electron with energy $\frac{1}{2} k_v^2$ is given by

$$\Gamma(R, k_v) = 2\pi |(\psi_r(\vec{r}, R) H_{e1} \psi_{k_v}^*(\vec{r}, R))|^2. \quad (15)$$

In order to simplify the nonlocal integral operators appearing in Eq. (10), one needs to assume^{26,27} that the electron kinetic energy $\frac{1}{2} k_v^2$ is large compared to the spacing between vibrational levels $\Delta W = W_{v+1} - W_v$, or alternatively, that the electronic matrix element in Eq. (14), and the width $\Gamma(R, k_v)$, depend weakly on the vibrational quantum number v . Thus, in the resonance region, one can replace $\frac{1}{2} k_v^2$ by the local electron kinetic energy $\frac{1}{2} k^2 = \epsilon_r(R) - \epsilon_0(R)$. If the closed vibrational channels make a negligible contribution to Eq. (10) (because of unfavorable Franck-Condon factors), then one can perform the sum over v to yield

$$\sum_v X_v(R) X_v^*(R') = \delta(R - R'). \quad (16)$$

Using Eqs. (14)–(16) in Eq. (10), we obtain the result

$$[E - \epsilon_r(R) - K_R] \xi_{v_i}(\vec{R}) = (\psi_r(\vec{r}, R) H_{e1} \psi_{k_i}^*(\vec{r}, R)) X_{v_i}(\vec{R}) + \left((2\pi)^{-1} \int \mathcal{P} dE' \frac{\Gamma(R, k')}{E - E'} - \frac{1}{2} i \Gamma(R, k_r) \right) \xi_{v_i}(\vec{R}). \quad (17)$$

Further, if the resonance wave function is dominated by a single partial wave [e.g., $l=2$ in case of $N_2(^2\Pi_g)$] then the electronic entry amplitude can be expressed in terms of the width:

$$(\psi_r(\vec{r}, R) H_{e1} \psi_{k_i}^*(\vec{r}, R)) = e^{i\delta_l(R)} (2\pi)^{-1/2} \Gamma(R, k_i)^{1/2}, \quad (18)$$

where $\delta_l(R)$ is the background phase shift for fixed nuclei. Finally, if $\delta_l(R)$ is a slowly varying func-

tion of R , one can incorporate the phase factor $e^{i\theta}$ into $\xi_{v_i}(\vec{R})$ and obtain the nuclear Schrödinger equation of the boomerang model

$$\begin{aligned} [E - K_r - \bar{\epsilon}_r(R) + \frac{1}{2}i\Gamma(R, k_r)]\xi_{v_i}(\vec{R}) \\ = (2\pi)^{-1/2}\Gamma(R, k_r)^{1/2}X_{v_i}(\vec{R}), \end{aligned} \quad (19)$$

where we have again replaced the incident momentum k_i by the local fixed-nuclei momentum k_r .

For convenience, the fixed-nuclei electronic "shift" is incorporated into the real part of the local complex potential $\bar{\epsilon}_r(R) - \frac{1}{2}i\Gamma(R, k_r)$ which determines the dynamics of the nuclei in the negative-ion compound state. Our main result, Eq. (19), is essentially identical to the formula used by Dubé and Herzenberg [see Eqs. (2.31) and (3.1) of Ref. 6]. Once the vibrational wave function of the resonance state $\xi_{v_i}(\vec{R})$ is determined, the transition amplitude for vibrational excitation can be calculated from the expression

$$T_{v_r v_i} = (2\pi)^{-1/2} \int d\vec{R} X_{v_r}^*(R) \Gamma(R, k_r)^{1/2} \xi_{v_i}(\vec{R}), \quad (20)$$

which is obtained from Eq. (1) by using Eqs. (6)–(8), (11), (14), and (18). To emphasize the physical assumptions underlying the complex-potential model, we summarize the approximations required in the derivation of Eq. (19) as follows:

- (1) The Born-Oppenheimer approximation is valid for the single isolated resonance or compound state.
- (2) The nonresonant background scattering can be described with the adiabatic nuclei wave functions.
- (3) The electronic coupling between the resonance state and the background continuum must be approximately independent of the ejected electron energy.
- (4) The energetically closed vibrational channels make a negligible contribution to the effective potential.
- (5) The background scattering is dominated by a single partial wave, and it is independent of internuclear distance in the Franck-Condon region.

III. CALCULATION OF FIXED-NUCLEI RESONANCE PARAMETERS FOR $N_2^-(^2\Pi_g)$

In the complex-potential or boomerang model, the vibrational-excitation cross section is calculated using the vibrational wave functions $X_{v_i}(\vec{R})$ of the target molecule and the corresponding function $\xi_{v_i}(\vec{R})$ associated with the negative-ion resonance state. In the case of N_2 , the former are determined by the electronic potential-energy curve $\epsilon_0(R)$ of the $^1\Sigma_g^+$ ground state of N_2 [see Eq. (13)]. On the other hand, the functions $\xi_{v_i}(\vec{R})$ are determined by the complex potential $\bar{\epsilon}_r(R) - \frac{1}{2}i\Gamma(R, k_r)$,

where $\bar{\epsilon}_r(R)$ and $\Gamma(R)$ are the electronic potential curve (including the shift) and the width, respectively, of the $^2\Pi_g$ resonance [see Eq. (19)]. In the present work, three different sets of $\epsilon_0(R)$, $\bar{\epsilon}_r(R)$, and $\Gamma(R)$ were used to test the sensitivity of the vibrational-excitation cross sections to these electronic parameters. However, in each case, the parameters were extracted from *ab initio* fixed-nuclei calculations of $N_2(^1\Sigma_g^+)$ and $N_2(^2\Pi_g)$.

A. R -matrix calculations of e - N_2 scattering

Recently, Schneider, LeDourneuf, and Vo Ky Lan¹¹ reported fixed-nuclei R -matrix calculations of e - N_2 scattering. The electron-molecule interaction was represented by a static-exchange potential; however, the polarization of N_2 was accounted for by constructing the potential from molecular orbitals, which were obtained from "stabilization self-consistent-field (SCF)" calculations²⁸ of $N_2^-(^2\Pi_g)$. This procedure allows for the distortion of the molecular charge distribution in the presence of the extra electron captured into a π_g orbital. For each internuclear distance R , the resonance parameters $\bar{\epsilon}_r$ and Γ were extracted by fitting the energy dependence of the $^2\Pi_g$ eigenphase sum $\delta(\epsilon)$ to the Breit-Wigner formula²⁹

$$\delta(\epsilon) - \delta_0 = \tan^{-1} \left(\frac{\Gamma/2}{\bar{\epsilon}_r - \epsilon} \right).$$

The background phase δ_0 was fitted to a second-order polynomial in ϵ . The resulting resonance energy and width (set I) are plotted as a function of R in Figs. 1 and 2, respectively. Figure 1 also shows the potential-energy curve of the ground $^1\Sigma_g^+$ state of N_2 which was obtained¹¹ using a single-configuration SCF wave function constructed from contracted Gaussian orbitals.

B. Stieltjes-moment theory calculations of N_2 resonance parameters

One direct method for calculating electronic resonance parameters is the Stieltjes-moment theory technique.³⁰ The resonance state $\psi_r(\vec{r}, R)$ is obtained as a square-integrable solution of an approximate Hamiltonian, and then $\Gamma(R)$ is calculated from the "golden-rule" formula, Eq. (15), using a discrete basis set representation of the background continuum.

Some time ago, one of us (A.U.H.) reported³⁰ $N_2^-(^2\Pi_g)$ resonance parameters which were calculated using this technique along with a frozen-core description of the resonance state. The ground state of N_2 was represented by a single-configuration SCF wave function. The wave function of the $^2\Pi_g$ resonance was constructed from a $^1\Sigma_g^+$ core, consisting of the frozen molecular orbitals of N_2 ,

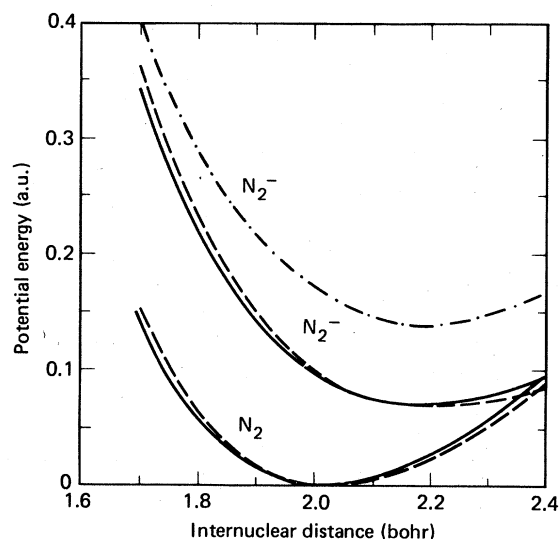


FIG. 1. Potential-energy curves of $N_2(^1\Sigma_g^+)$ and $N_2(^2\Pi_g)$. Solid lines: R -matrix calculation with polarized core (set I from Ref. 11); dot-dashed line: Stieltjes calculation with frozen core (set II from Ref. 30); dashed lines: Stieltjes calculation with polarized core (set III, present work).

and an optimized π_g orbital describing the captured electron. The $k\pi_g$ background continuum was represented by 14–16 symmetry adapted molecular orbitals. Since in this approximation the polarization of N_2 was ignored, the calculation was essentially equivalent to a static-exchange treatment of the e - N_2 interaction, and the calculated resonance energies and widths³⁰ compared favorably with

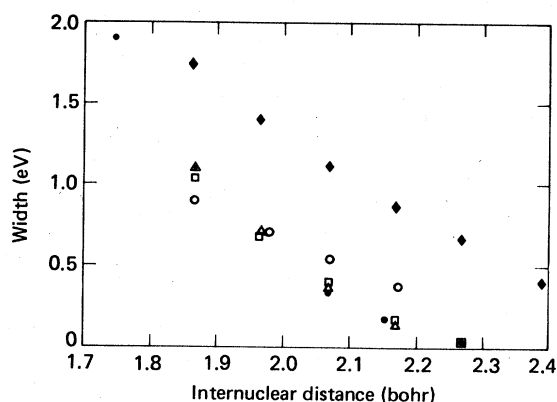


FIG. 2. Electronic width of $N_2(^2\Pi_g)$ as a function of internuclear distance. \bullet R -matrix calculation with polarized core (set I from Ref. 11). \blacklozenge Stieltjes calculation with frozen core (set II from Ref. 30). \square Stieltjes calculation with polarized core (set III, present work). \triangle T -matrix calculation with polarized core (from Ref. 33). \circ semiempirical results of Dubé and Herzenberg (from Ref. 6).

those obtained in other static-exchange calculations.^{31–33} The resonance parameters $\bar{\epsilon}_r(R)$ and $\Gamma(R)$ obtained with the Stieltjes technique and the frozen-core model (set II) are also shown in Figs. 1 and 2.

One advantage of the Stieltjes method is that electron correlation and polarization effects are easily incorporated into the calculation of the resonance parameters, since the method relies on square-integrable basis functions exclusively. In the present work, we also calculated resonance wave functions which were represented by linear combinations of configurations among which we include all single excitations from the $2\sigma_g$, $2\sigma_u$, $1\pi_u$, and $3\sigma_g$ core orbitals to the unoccupied orbitals. Our one-electron basis consisted of $9\sigma_g$, $9\sigma_u$, $19\pi_g$, and $6\pi_u$ orbitals, and the total number of configurations was 193. The nonresonant $^2\Pi_g$ background continuum was again represented by simple products of the frozen $^1\Sigma_g^+$ core and the $n\pi_g$ orbitals ($n = 4, \dots, 19$). This model allows for the distortion and spin polarization³⁴ of the N_2 target while the scattering electron is close to the molecule, i.e., while it is captured in the π_g resonance orbital, but no polarization is included for nonresonant scattering. The resulting resonance energies and widths (set III) are plotted as a function of R in Figs. 1 and 2, respectively. As Fig. 2 shows, our configuration-interaction treatment of target polarization yields widths that agree well with the widths obtained in the R -matrix¹¹ and T -matrix³³ calculations which utilized the static-exchange model along with the stabilization-SCF procedure²⁸ instead. To facilitate the presentation and the discussion of the computed vibrational-excitation cross sections in Sec. IV, Table I summarizes the three sets of fixed-nuclei electronic resonance parameters employed in our work.

IV. CALCULATED CROSS SECTIONS

Here we compare our calculated cross sections for N_2 to some previous theoretical and experimental data. We also examine the effects of target polarization and the dependence of the cross sections on the various fixed-nuclei electronic resonance parameters employed in the complex-potential model.

A. Effects of polarization

Previous theoretical studies^{9–11,16} of e - N_2 scattering already established that polarization of N_2 by the incoming electron must be accounted for in order to obtain resonant behavior of the vibrational-excitation cross section in the experimentally observed energy range, 1.5–4.5 eV. Our results

TABLE I. Summary of fixed-nuclei electronic resonance parameters of $N_2^-(^2\Pi_g)$ used in the complex-potential model. Energies and widths are in eV and $R_0=2.068$ bohr.

Name	Type of calculations	Target polarization	$\bar{\epsilon}_r(R_0)^a$	$\Gamma(R_0)$
Set I	R -matrix ^b stabilization—SCF on N_2^-	Yes	2.15	0.34
Set II	Stieltjes—imaging ^c frozen N_2 core	No	4.13	1.14
Set III	Stieltjes—imaging ^d configuration interaction	Yes	2.23	0.40

^a Resonance energy relative to the energy of N_2 at 2.068 bohr.

^b Schneider, LeDourneuf, and Vo Ky Lan, Ref. 11.

^c Hazi, Ref. 30.

^d Present work.

fully confirm this conclusion. Table I clearly shows that the resonance energy and the width of the $N_2^-(^2\Pi_g)$ state calculated without polarization (set II) are much larger than the corresponding parameters obtained by including target distortion (sets I or III). For internuclear distances between 1.7 and 2.4 bohr, the potential-energy curve of N_2^- obtained with the frozen-core model is too high in energy by 1.7–2.0 eV (see Fig. 1), whereas the corresponding width is too large by 0.4–0.5 eV (see Fig. 2). Figure 3 compares the integrated vibrational-excitation cross sections for the 0–1 and 0–2 transitions in N_2 which were calculated with resonance parameters I and II. In the frozen-core static-exchange model the excitation cross sections are enhanced only for electron energies above 3.5 eV and show no substructure, in contrast to the experimental results.^{1,3} On the other hand, when the distortion of the target molecule by the incoming electron is included in the *ab initio* calculation of the resonance parameters, the excitation cross sections exhibit the characteristic substructure in the experimentally observed¹ energy

region between 1.5 and 4.5 eV and also have the correct magnitude.^{3,11}

It is worth emphasizing that the way we treated target polarization in our calculations is quite different from the usual procedure of employing a semiempirical dipole polarization potential^{35,36} which behaves asymptotically like α/r^4 . In the single-excitation–configuration-interaction calculation (see Sec. III B), it is the short-range distortion of the molecular charge distribution which is explicitly included by allowing the individual molecular orbitals to relax in the presence of the temporarily captured π_g electron. The stabilization-SCF procedure^{11,28} accomplishes essentially the same effect. Neither of these two methods takes into account the long-range dipole polarization potential. Recently, Levin and McKoy³³ have also argued that short-range distortion of the target should be the most important effect for scattering channels exhibiting shape resonances. The realistic resonant vibrational-excitation cross sections, which have been obtained for N_2 in the present *ab initio* calculations and in Ref. 11, support this argument.

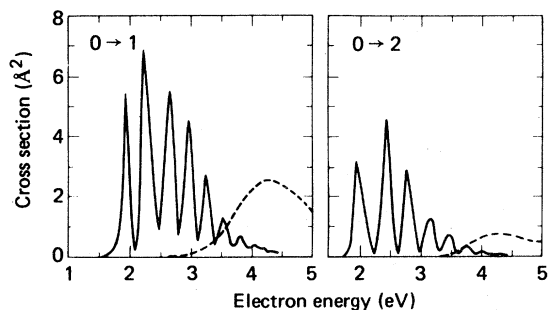


FIG. 3. Effect of target polarization on the 0–1 and 0–2 vibrational-excitation cross sections. Solid lines: Results obtained with polarized core (set I); dashed lines: Results obtained with frozen core (set II).

B. Comparison of complex-potential model and R -matrix results

One of the primary objectives of our study was to test the validity of the physical assumptions underlying the complex-potential or boomerang model. We have done this by comparing in detail our calculated cross sections for the vibrational excitation of N_2 to those obtained recently with the R -matrix method^{11,12} in which neither the existence of a local resonance width $\Gamma(R)$, nor the weak dependence of the nonresonant scattering on internuclear separation were explicitly assumed. To make the comparison meaningful, we computed the boomerang cross sections using the resonance parameters

(set I) which were extracted from the fixed-nuclei R -matrix eigenphases¹¹ (see Sec. III A).

Figure 4 compares the calculated vibrational-excitation cross sections for the $0 \rightarrow v$, $v=1-4$ transitions in N_2 . The absolute magnitudes of the cross sections, as well as the number, the shapes, and the relative positions of the peaks given by the two methods agree closely. The agreement is especially noteworthy for the higher cross sections, e.g., the unusual shapes of the 2.2 eV peak in the $0 \rightarrow 2$ and $0 \rightarrow 3$ cross sections are faithfully reproduced in both the boomerang and R -matrix calculations. We conclude from these results that the assumption of a local resonance width in the complex-potential model is justified for the ${}^2\Pi_g$ resonance of N_2^- .

The largest differences between the two calculations are found for the $0 \rightarrow 1$ cross section, but the origin of this discrepancy is not understood. Possibly it is due to neglecting the dependence of the nonresonant background π_g eigenphase on internuclear distance in the boomerang model. This eigenphase certainly contributes to the vibrationally elastic, e.g., $0 \rightarrow 0$ cross sections, but its role in vibrational excitation is not at all established. Alternatively, the differences in $0 \rightarrow 1$ cross sections may be due to using slightly different Morse potentials to represent the N_2^- potential-energy curves in the two calculations. As the re-

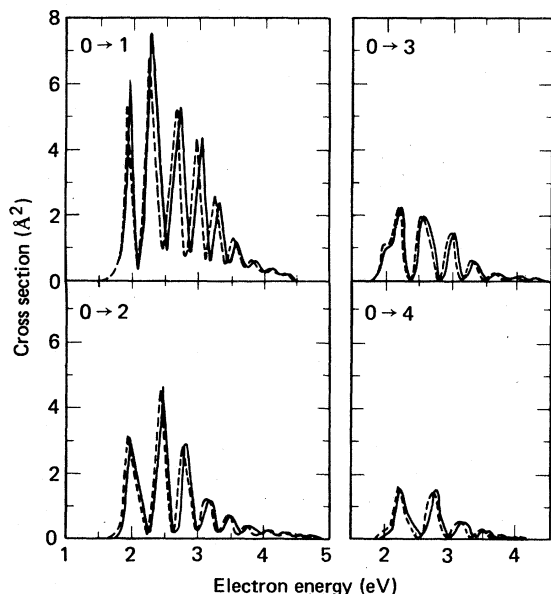


FIG. 4. Comparison of vibrational-excitation cross sections obtained with the complex-potential or boomerang model and with the R -matrix method. Solid lines: R -matrix calculation of Schneider, LeDourneuf, and Vo Ky Lan (Ref. 11); dashed lines: Boomerang calculation with *ab initio* resonance parameters (set I).

sults of the following section will show, the detailed structure of the computed cross sections is quite sensitive to this particular resonance parameter.

C. Dependence of the cross sections on the fixed-nuclei resonance parameters

Before the recent *ab initio* studies of resonant vibrational excitation of N_2 were completed, Dubé and Herzenberg had argued⁶ that extremely accurate resonance parameters of the temporary negative ion would be required to obtain vibrational-excitation cross sections which had the right magnitude and which had peaks at the correct energies. Furthermore, they asserted that only semiempirical procedures, employing adjustable resonance parameters, could meet this strict requirement and be practicable. Although our work clearly shows that using *ab initio* fixed-nuclei resonance parameters in the complex-potential model can provide satisfactory vibrational-excitation cross sections, it seems worthwhile to investigate the dependence of the computed cross sections on the accuracy of the electronic resonance energy and the width.

Figure 5 compares two sets of vibrational-excitation cross sections which were calculated with the boomerang model for the $0 \rightarrow 1$ and $0 \rightarrow 3$ transitions employing different sets of fixed-nuclei resonance parameters. In one case we used the potential-energy curves and the resonance widths extracted from the fixed-nuclei R -matrix calculations¹¹ (set I). In the other case we used the results of our configuration-interaction study (set III). However, both sets of electronic resonance parameters included the effects of target polarization. Figure 5 shows that, although the two sets of cross sections

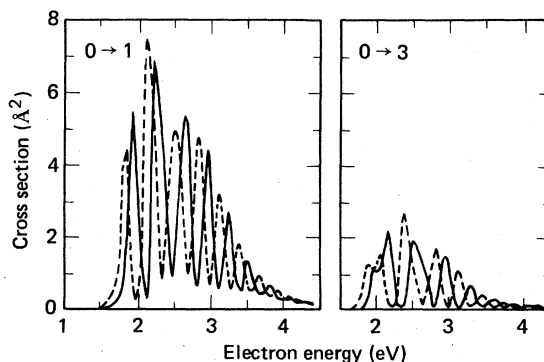


FIG. 5. Comparison of vibrational-excitation cross sections calculated with the boomerang model using different sets of *ab initio* resonance parameters. Solid lines: Results obtained with set I; dashed lines: Results obtained with set III.

have very similar magnitudes, the corresponding individual peaks are shifted relative to each other by about 0.15 eV. This shift is due solely to small differences in the potential-energy curves obtained in the present and the previous¹¹ calculations. As Fig. 1 shows, the two fixed-nuclei calculations which take into account target polarization predict essentially the same energy difference between the minima in the potential-energy curves of N_2 and N_2^- . However, the curves of both N_2 and N_2^- resulting from the R -matrix study are tilted slightly toward smaller internuclear distances. These results indicate that the detailed structure in the computed vibrational-excitation cross sections is sensitive to the potential-energy curves of both N_2 and N_2^- , as Dubé and Herzberg⁶ had found earlier.

We also checked the dependence of the cross sections on the resonance width by doing two calculations with the same potential-energy curves (set I) but with different widths (sets I and III). In this case, the peaks in the cross sections occurred at the same energy but had slightly different magnitudes. This confirms the expectation that the resonance width mainly determines the size of the vibrational-excitation cross sections. Of course, when the width becomes too large, the detailed structure in the cross section disappears (see Sec. IV A).

Finally, it is worth noting in Fig. 2 that the width derived by Dubé and Herzberg in their semiempirical study⁶ differs from those obtained in the various *ab initio* calculations^{11,33} in two respects, it is about 50% larger at $R=2.068$ bohr, and it has a substantially smaller, negative slope. Nevertheless both the semiempirical and the *ab initio* resonance parameters produce realistic vibrational-excitation cross sections when used in the boomerang model. This suggests that there may not be a unique set of fixed-nuclei resonance parameters which give correct cross sections, and that caution should be used in extracting molecular resonance parameters directly from experimental data.

D. Comparison with experimental results

Here we compare our calculated cross sections for N_2 to experimentally determined absolute cross sections: The differential cross section for vibrational excitation³ at 90° , and the total cross section for the ground vibrational state.^{2,10} Since all the theoretical cross sections presented so far have been integrated cross sections, we briefly discuss the calculation of differential cross sections in the complex-potential or boomerang model. Dubé and Herzberg⁶ showed that, for

resonant vibrational excitation, $d\sigma/d\Omega$ has the simple form

$$\frac{d\sigma_{i \rightarrow f}}{d\Omega} = g(\theta)\sigma_{i \rightarrow f}, \quad (21)$$

where $\sigma_{i \rightarrow f}$ is the integrated cross section and $g(\theta)$ is the normalized angular distribution, independent of energy. In the case of $N_2(^2\Pi_g)$, a single partial wave (d wave) dominates the resonant scattering and $g(\theta)$ takes the form

$$g(\theta) = (4\pi)^{-1} \frac{15}{14} (1 - 3 \cos^2 \theta + \frac{14}{3} \cos^4 \theta). \quad (22)$$

Until recently the correct normalization of the vibrational-excitation cross sections for N_2 was quite uncertain, as different experiments^{1,3} yielded results which differed by as much as a factor of 4. However, the most recent theoretical works^{9,11} all favor the normalization implied by the latest experiments of Wong *et al.*,³ who measured the absolute differential cross sections at 90° for the $0-1$ and $0-2$ transitions. Figure 6 compares the differential cross sections calculated with the fixed-nuclei resonance parameters (set I) to the experimental results. Although the overall magnitudes of the experimental and the computed cross sections compare favorably, the relative heights and the positions of the peaks are not quite the same. But considering the sensitivity of the computed cross sections to the electronic potential-energy curves, which we have demonstrated in Sec. IV C, the agreement between theory and experiment is satisfactory. The present *ab initio* calculations confirm the normalization of the experimental data of Wong *et al.*³

It is clear from Fig. 6 that the higher peaks in the computed cross sections are shifted to higher energies relative to the experimental ones. This is probably due to the single-configuration SCF representation of the $X^1\Sigma_g^+$ state of N_2 , employed in all three *ab initio* calculations (see Sec. III). It is known³⁷ that SCF calculations on the electronic ground state of N_2 yield only 50–55% of the true dissociation energy, and that they predict incorrect vibrational frequencies and anharmonicities. There is every reason to believe that using a more accurate description of $N_2(^1\Sigma_g^+)$, (for example, a multiconfiguration-SCF wave function) in the fixed-nuclei calculations would yield improved vibrational-excitation cross sections.

In order to calculate the total cross section for the ground state of N_2 , we have summed the $0-v$ cross sections up to $v=10$, and included a constant, 10 \AA^2 cross section to represent the contribution of the nonresonant symmetries.³⁸ Figure 7(b) compares the total cross sections obtained in

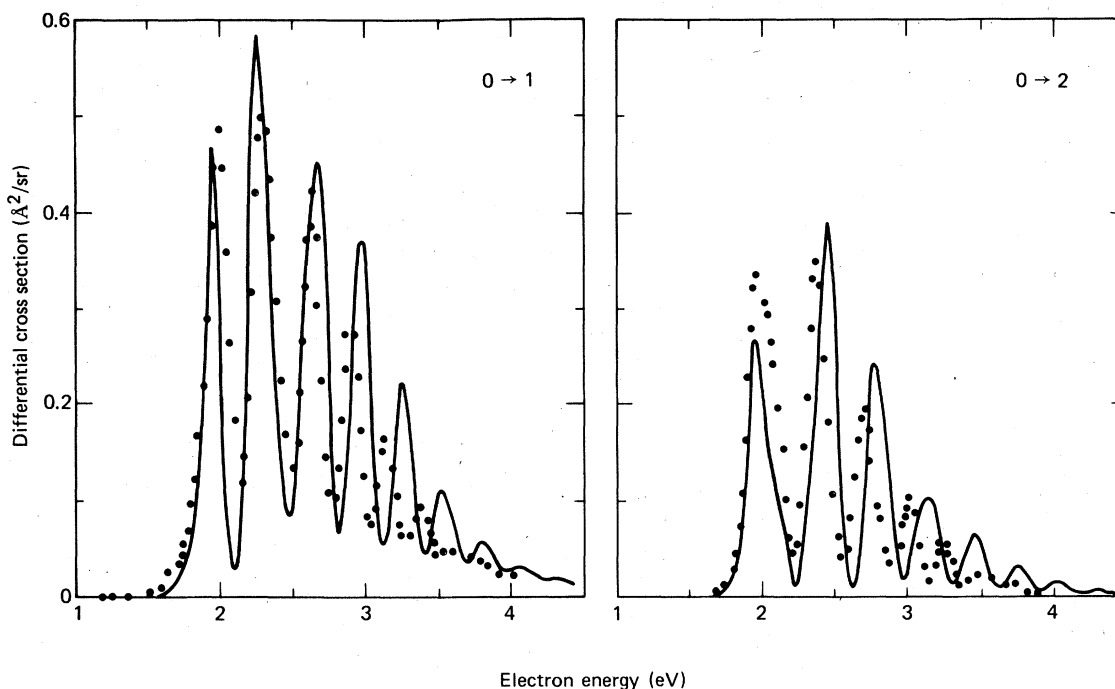


FIG. 6. Comparison of theoretical and experimental differential cross sections for vibrational excitation of N_2 at 90° . Solid lines: Boomerang calculations with resonance parameters (set I). Dots: Experimental data of Wong *et al.* (Ref. 3).

this way to the experimental data of Kennerly,² which agree well with the earlier results of Golden.¹⁸ The computed cross section is clearly much too large for energies less than 3 eV. Essentially the same difficulty plagued the semi-empirical calculations of Dubé and Herzenberg (see Fig. 5 of Ref. 6).

By comparing our individual cross sections to those obtained in the R -matrix calculations¹¹ we find that the discrepancy is due solely to the vibrationally elastic $0-0$ cross section, which is predicted to be too large even when the correct *ab initio* resonance parameters (set I) are employed. We believe that the difficulty arises because the T -matrix formula in the boomerang model, Eq. (20), does not have the correct energy dependence near threshold, i.e., as $k_f \rightarrow 0$. In the case of N_2 , this defect does not affect appreciably the vibrational-excitation cross sections because they are negligible for energies less than 1.5 eV, but it leads to a significant overestimation of vibrationally elastic cross sections at low electron energies. To verify this hypothesis, we have recalculated the total cross section using an energy-modified $0-0$ cross section which was computed with the following exit amplitude:

$$(2\pi)^{1/2}(\psi_r(\vec{r}, R)H_{el}\psi_{k_f}^+(\vec{r}, R)) = \Gamma(R, k_r)^{1/2}, \quad k_f > k_r \quad (23a)$$

$$= \Gamma(R, k_r)^{1/2}(k_f/k_r)^{5/2}, \quad k_f < k_r. \quad (23b)$$

The expression in Eq. (23b) is somewhat arbitrary, but its threshold behavior is appropriate for a π_g channel. As Fig. 7(a) shows, the agreement between theory and experiment is much more satisfactory when the energy-modified $0-0$ cross section is used. These results indicate that, in the case of N_2 , the original boomerang model^{5,6} yields vibrationally elastic cross sections which are much less satisfactory than the corresponding excitation cross sections.

V. CONCLUSIONS

We have used the complex-potential or boomerang model^{5,6} to calculate cross sections for the resonant vibrational excitation of N_2 by low-energy electrons. The electronic resonance parameters required in the model were extracted from *ab initio* fixed-nuclei calculations of the ${}^2\Pi_g$ resonance state of N_2^- , with no adjustable parameters. We

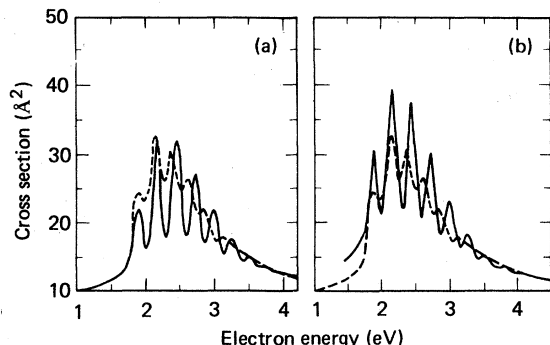


FIG. 7. Comparison of theoretical and experimental total cross sections for the $v=0$ level of N_2 . Solid lines: Boomerang model using *ab initio* resonance parameters (set I); dashed lines: Experimental results of Kennerly (Ref. 2). (a) Theoretical results obtained with an energy modified elastic ($0-0$) cross section, (b) theoretical cross section contains an unmodified elastic component.

have examined in detail the physical assumptions required to derive the complex-potential model for describing the motion of the nuclei in resonant electron-molecule collisions. The good agreement between the present vibrational excitation cross sections and those obtained by Schneider, LeDourneuf, and Vo Ky Lan in their R -matrix calculations¹¹ indicates that the assumption of a local energy-independent resonance width $\Gamma(R)$ is justified in the case of $N_2(^2\Pi_g)$. Since the cross section formula in the complex-potential model does not have the correct energy dependence near threshold, the model overestimates the vibration-

ally elastic cross sections.

We have also shown that, in order to obtain realistic vibrational-excitation cross sections showing the experimentally observed structure, the electronic resonance parameters must be calculated in such a way as to account for the short-range distortion or polarization of the N_2 target. By comparing the cross sections calculated with different electronic resonance parameters, we have found that the positions and the relative heights of the peaks in the cross section are rather sensitive to the potential-energy curve of the temporary negative ion. On the other hand, the magnitudes of the computed cross sections are controlled mostly by the fixed-nuclei resonance width.

Our differential vibrational-excitation cross sections, calculated at 90° , confirm the normalization of the experimental data of Wong *et al.*³ The total cross section calculated with an energy-modified $0-0$ cross section agrees reasonably well with the experimental data^{2,18} available for the ground vibrational state.

ACKNOWLEDGMENTS

We thank Professor N. Bardsley, Professor S. F. Wong, and Dr. B. Schneider, Dr. M. LeDourneuf, and Dr. Vo Ky Lan for sending us their data on N_2 prior to publication. This work was performed under the auspices of the U. S. Department of Energy by the Lawrence Livermore National Laboratory under Contract No. W-7405-Eng-48.

¹G. J. Shulz, in *Principles of Laser Plasmas*, edited by G. Bekefi (Interscience, New York, 1976).

²R. E. Kennerly, *Phys. Rev. A* **21**, 1876 (1980).

³S. F. Wong, J. A. Michejda, and A. Stamatovic (unpublished).

⁴For a review see, B. L. Moiseiwitsch, *Rep. Prog. Phys.* **40**, 843 (1977).

⁵D. T. Birtwistle and A. Herzenberg, *J. Phys. B* **4**, 53 (1971).

⁶L. Dubé and A. Herzenberg, *Phys. Rev. A* **20**, 194 (1979).

⁷R. K. Nesbet, *Phys. Rev. A* **19**, 551 (1979).

⁸W. Domcke and L. S. Cederbaum, *Phys. Rev. A* **16**, 1465 (1977).

⁹N. Chandra and A. Temkin, *Phys. Rev. A* **13**, 188 (1976); **14**, 507 (1976).

¹⁰A. Temkin, in *Electron-Molecule and Photon-Molecule Collisions*, edited by T. Rescigno, V. McKoy, and B. Schneider (Plenum, New York, 1979), p. 173.

¹¹B. I. Schneider, M. LeDourneuf, and Vo Ky Lan, *Phys. Rev. Lett.* **43**, 1926 (1979).

¹²B. I. Schneider, M. LeDourneuf, and P. G. Burke, *J.*

Phys. B **12**, L365 (1979).

¹³For a review of recent applications of the boomerang model to vibrational excitation and dissociative attachment, see N. Bardsley, in *Electron-Molecule and Photon-Molecule Collisions*, edited by T. Rescigno, V. McKoy, and B. Schneider (Plenum, New York, 1979), p. 267.

¹⁴F. Fiquet-Fayard, *Vacuum* **24**, 533 (1974).

¹⁵A. Temkin, *Comments At. Mol. Phys.* **6**, 27 (1976).

¹⁶For example, see P. G. Burke and N. Chandra, *J. Phys. B* **5**, 1696 (1972); P. G. Burke and B. D. Buckley, *ibid.* **10**, 725 (1977).

¹⁷A. Temkin (private communication).

¹⁸D. E. Golden, *Phys. Rev. Lett.* **17**, 847 (1966).

¹⁹A. Herzenberg, *J. Phys. B* **1**, 548 (1968).

²⁰J. N. Bardsley, A. Herzenberg, and F. Mandl, *Proc. Phys. Soc. London* **89**, 305 (1966); **89**, 321 (1966).

²¹T. F. O'Malley, *Phys. Rev.* **150**, 14 (1966).

²²For an alternative derivation of Eq. (10), see Ref. 13.

²³E. S. Chang and A. Temkin, *Phys. Rev. Lett.* **23**, 399 (1969); F. H. M. Faisal and A. Temkin, *ibid.* **28**, 203 (1972).

- ²⁴M. Shugard and A. U. Hazi, *Phys. Rev. A* **12**, 1895 (1975).
- ²⁵To simplify the formalism, we neglect the rotational motion of the nuclei throughout the paper.
- ²⁶J. N. Bardsley, *J. Phys. B* **1**, 349 (1968).
- ²⁷R. J. Bieniek, *J. Phys. B* **13**, 4405 (1980).
- ²⁸M. Krauss and F. H. Mies, *Phys. Rev. A* **1**, 1592 (1970).
- ²⁹A. U. Hazi, *Phys. Rev. A* **19**, 920 (1979).
- ³⁰A. U. Hazi, in *Electron-Molecule and Photon-Molecule Collisions*, edited by T. Rescigno, V. McKoy, and B. Schneider (Plenum, New York, 1979), p. 281.
- ³¹M. A. Morrison and B. I. Schneider, *Phys. Rev. A* **16**, 1003 (1977).
- ³²L. A. Collins, W. D. Robb, and M. A. Morrison, *J. Phys. B* **11**, L777 (1978).
- ³³D. A. Levin and V. McKoy (unpublished).
- ³⁴H. F. Schaefer, *The Electronic Structure of Atoms and Molecules* (Addison-Wesley, Menlo Park, 1972), p. 122.
- ³⁵N. F. Lane, *Rev. Mod. Phys.* **52**, 1 (1980).
- ³⁶D. G. Truhlar, in *Electron-Molecule and Photon-Molecule Collisions*, edited by T. Rescigno, V. McKoy, and B. Schneider (Plenum, New York, 1979), p. 151.
- ³⁷See, for example, W. Butscher, S. Shih, R. J. Buenker, and S. D. Peyerimhoff, *Chem. Phys. Lett.* **52**, 457 (1977).
- ³⁸This value is consistent with the vibrationally elastic component calculated in Ref. 9 for the ${}^2\Sigma_g^+$, ${}^2\Sigma_u^+$, and ${}^2\Pi_u$ symmetries.